Journal of Innovative Optical Health Sciences
Vol. 7, No. 3 (2014) 1450021 (8 pages)

DOI: 10.1142/S1793545814500217

The accurate localization of fluorescent nanoparticle Au–Ft in *nu/nu* mice kidney

Hui Yang*,§, Cuiji Sun†, Jun Jia‡, Guangjun Nie†
and Zhenyu Wu*
*Department of Immunology, Guang'anmen Hospital, P. R. China
Academy of Chinese Medical Sciences, Beijing 100053, P. R. China
†CAS Key Laboratory for Biomedical
Effects of Nanomaterials & Nanosafety
National Center for Nanoscience and Technology
Beijing 100190, P. R. China
‡Chilong Healthcare International Limited
Beijing 100070, P. R. China
§yanghui1517@163.com

Received 4 September 2013
Accepted 1 December 2013
Published 9 January 2014

Au–Ft, as a green synthesized nanoparticle, is composed of a ferritin nanocage enclosing a pair of Au nanoclusters inside. Our previous study has demonstrated that Au–Ft can be an excellent fluorescent probe for whole body imaging of mice with kidney specific targeting. But, the accurate localization of Au–Ft in kidney is still absent. In the current study, we detected and assessed the cellular and subcellular localization of Au–Ft in renal cortex and medulla of *nu/nu* mice after tail vein injection by using Nuance optical system (CRi, Woburn, USA) and inForm intelligent image analysis software based on single cell segmentation. We obtained the fluorescence intensity and cellular location of kidney-targeting Au–Ft probe in particular cell of renal glomerulus or renal tubules, which provided valuable proofs to clarify the mechanism of Au–Ft selective enrichment in kidney and the associated metabolic processes.

Keywords: Au–Ft nanoparticle; kidney targeting; cellular localization; renal cortex and medulla; multispectral imaging.

1. Introduction

Various nanostructures have shown great promise in biomedical imaging, biosensing, drug delivery and disease diagnostics. Due to the unique intrinsic photoluminescence, gold clusters below 2 nm in diameter have attracted great attention. Ferritin is

a "nanocage-type" protein composed of 24 domains with outer diameter of 13 nm. In previous work,[1] we obtained Au–Ft nanostructure by assembling two gold nanoclusters within ferritin heavy chains. Au–Ft retained noble metal's intrinsic fluorescence properties in the far-red region, and could be used as a fluorescent probe for *in vivo* imaging, with specific tissue-targeting ability for the kidney of *nu/nu* mice. The accurate localization of Au–Ft in kidney is necessary to be further explored to interpret the underlying mechanism for its kidney uptake as well as the associated metabolic processes.

For different scales of nanoparticles into systemic circulation, their distribution and metabolism *in vivo* has caused widespread concerns.[2] The kidney is an important metabolic organ, in which the substances in the blood undergo several transport processes including glomerular filtration, tubular reabsorption and/or tubular secretion, being excreted with urine or going back to systemic circulation.[3,4] For example, glucose and amino acid could be completely reabsorbed at kidney tubules, electrolyte and water are mostly reabsorbed, creatinine is not reabsorbed.[5,6] As to nanoparticle, little is known about these processes. The cutoff size for efficient kidney excretion of nanoparticles is approximately 5.5 nm,[7] which indicated that nanoparticles with diameter less than 5.5 nm would penetrate glomerular capillary wall into urine or/and be secreted by renal tubular cells into the urine. According to studies exploring the size-dependent biodistribution of nanoparticles for kidney accumulation, nanoparticles with a diameter less than 20 nm indeed could be found in kidney, though the accumulated amount in kidney was not significant in most studies.[8–10] However, the metabolic pathway and specific accumulation region of nanoparticles in kidney remained obscure. Au–Ft with diameter of 13 nm possesses far-red fluorescence emission, and has been confirmed to be enriched obviously in the kidney,[1] so it could be used as a modeling material to explore the distribution and localization of nanoscale particles within the kidney.

Multispectral imaging technology has been used to acquire images at many wavelengths to determine fluorophore distribution in cells or tissues. It permits the analysis of tissue with greater spectral densities and resolution of varied overlapping chromogens. One of the major limitation of some automated systems is its inability to segment tissue into nuclear and cytoplasmic areas, especially when there is strong intense histochemical staining.[11,12] The commercially available Nuance system from CRi (Woburn, Massachusetts, USA) could potentially help fill this gap, as its multispectral capabilities have the ability to separate visual components to demarcate different cellular components.[13] Tissue-based cytometric analysis could be performed using multispectral imaging technology in combination with inForm, an image analysis software which would help to obtain per-cell and per-cell-compartment multiparameter data.

In this study, we will explore the accurate cellular and tissue location of Au–Ft on kidney tissue section by using Nuance imaging and imaging analysis system. Through labeling cell membrane and nucleus with specific fluorescent probe, inForm (Nuance, CRi) may quantitate Au–Ft fluorescence signal located on cell membrane or nucleus from autofluorescence in the corresponding cells regions. InForm may also extract flow-cytometry-like data while preserving the morphological context of cell and tissue. Through these work, we could obtain the Au–Ft signal intensity and distribution profiles in both renal cortex and renal medulla regions on tissue and cellular levels.

2. Methods

2.1. *Synthesis and characterization of Au–Ft nanoparticles*

Au–Ft was synthesized as previously reported,[1] in which the ferroxidase active sites of apoferritin were used as bioreactors to synthesize Au clusters inside a ferritin nanocage. The concentration of ferritin protein was measured by the bicinchoninic acid (BCA) method. The excitation and emission spectrum were determined by using Hitachi F-4500 fluorescence spectrophotometer (Hitachi High-Technologies Corporation, Tokyo, Japan).

2.2. *Administration of Au–Ft on nu/nu mice and preparation of kidney sections*

All animal experiments were approved by the Animal Ethics Committee of the Medical School, Beijing University. Female *nu/nu* mice (8 weeks, $20 + 2$ g) obtained from Beijing Vital River laboratories were injected via the tail vein with the Au–Ft

probe (0.28, 0.4 or 0.5 nmol ferritin protein/g body weight; same as 2.8, 4 or 5 μmol ferritin protein/L blood) diluted in 0.9% NaCl solution. About 5 h after injection, mice were sacrificed, kidneys were fixed and embedded in paraffin blocks and sagittal sectioned at 5 μm. Slides were dewaxed before imaging or labeling with other fluorescent probe/fluorochrome.

2.3. *Imaging of HE stained kidney sections*

Hematoxylin-eosin (H&E) staining was performed on kidney sections with or without Au–Ft treatment. Bright-field imaging of these sections were acquired on an Olympus IX71 Inverted Microscope equipped with a Sony DXC-390P color CCD camera.

2.4. *Fluorescent labeling of cell membrane and nucleus on kidney sections*

To detect the accumulation of Au–Ft on cell membrane, cytoplasm and nucleus, DAPI and Dio (3,3′-dioctadecyloxacarbocyanine perchlorate, a lipophilic carbocyanine dye labeling cell membranes) were used to identify the position of nucleus and cell membrane, respectively. Blank-labeling kidney sections were prepared from *nu/nu* mice kidney without any fluorescence reagent treatment. Au–Ft single-labeling kidney sections were prepared from mice kidney with Au–Ft administrated by tail vein injection (5 μmol ferritin protein/L blood). Dewaxed kidney sections without Au–Ft treatment were stained by DAPI (5 μg/mL) or Dio (50 μmol/L) to obtain the DAPI or Dio single-labeling sections. Triple-labeling kidney sections were obtained by counterstaining kidney section with Au–Ft treatment with Dio (50 μmol/L) and DAPI (5 μg/mL) in turn.

2.5. *Quantitative image analysis*

The kidney sections were examined via an inverted fluorescence microscope (Olympus IX71 Inverted microscope, Olympus Corporation, Tokyo, Japan) equipped with a Nuance multispectral imaging system (CRi, Woburn, MA). To obtain the Au–Ft signal, excitation and emission filters were set at 510–550 nm and 590 nm LP, respectively; for Dio signal, the excitation and emission filters were set at 450–480 nm and 515 nm LP, respectively; for DAPI signal, the excitation and emission filters were set at 330–385 nm and 420 nm LP, respectively. The liquid crystal tunable emission filter was automatically stepped in 10 nm increments from 580 to 680 nm for Au–Ft, from 500 to 600 nm for Dio, from 420 to 540 nm for DAPI. The CCD captured images at each wavelength with constant exposure.

Multispectral imaging captures information from multiple wavelengths instead of simply the red, green and blue that human eyes see, the spectra of eachpixel were collected. The autofluorescence signal of blank kidney sections were obtained at different excitation/emission wavelength corresponding to Au–Ft, Dio or DAPI, single-labeling kidney slide were scanned to acquire the mixed signals of Au–Ft (Dio or DAPI) and autofluorescence, then these spectra data were dealt by using "compute pure spectrum" method (patent number: US 6930773 B2) to obtain the pure spectra of Au–Ft, Dio and DAPI. The pure spectra were then applied on multi-labeling fluorescence imaging to achieve fluorescent signal unmixing and ubiquitous autofluorescence removal. Intelligent image analysis software inForm could perform tissue segmentation and cell segmentation. By identification of the subcellular structure with specific cell membrane (Dio) and nucleus (DAPI) fluorescent probes, Au–Ft fluorescence signal could be quantitated at different cellular regions as per-cell and per-cell-compartment data.

2.6. *Statistic analysis*

The fluorescent intensity data are presented as means $\pm$ standard deviation (SD). Statistical significance in the differences between different groups was evaluated by LSD t-tests or Tukey's method after analysis of variance (ANOVA).

3. Results and Discussion

3.1. *Spectra characterization of Au–Ft*

The excitation and emission spectra of Au–Ft were measured, showing that the optimal excitation wavelength was 365 nm, while the maximum emission wavelength was 655 nm, which were fairly in agreement with the spectroscopic characteristics of Au–Ft.[1]

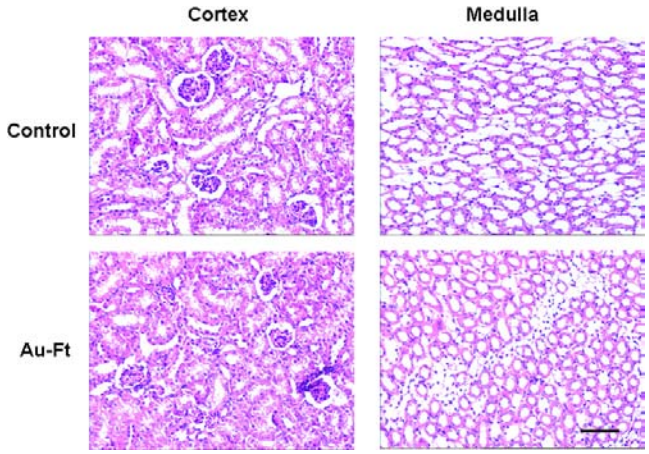

Fig. 1. Histological analysis of the kidney of *nu/nu* mice after Au–Ft treatment. Au–Ft (final blood concentration 5.0 μmol/L) or saline control were injected into *nu/nu* mice. About 5 h after the treatment, mice were sacrificed, organs were fixed and embedded in paraffin blocks and sectioned at 5 μm. The bright-field images of H&E staining sections were acquired with an Olympus IX71 Inverted microscope equipped with a Sony DXC-390P color CCD camera. The scale bar is 200 μm.

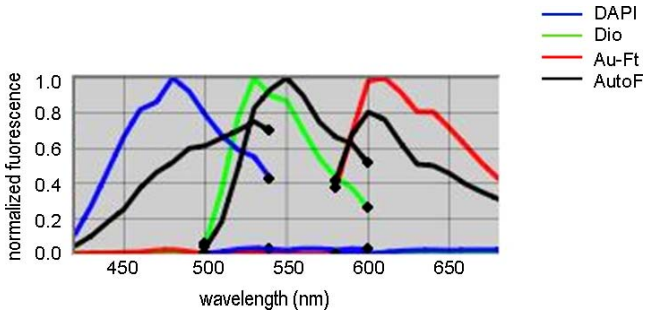

Fig. 2. Fluorescent probe emission spectra and tissue autofluorescence data used for spectral deconvolution. Tissue slices labeled with one kind of fluorescent probe were examined via an inverted fluorescence microscope (Olympus IX71 Inverted microscope, Olympus Corporation, Tokyo, Japan) equipped with a Nuance multispectral imaging system (CRi, Woburn, MA). To obtain the Au–Ft, Dio and DAPI signal, excitation and emission filters were set at 510–550 nm/590 nm LP, 450–480 nm/515 nm LP, 330–385 nm/420 nm LP, respectively. "Compute pure spectrum" method (patent number: US 6930773 B2) was used on unmixing Au–Ft (Dio or DAPI) signals and tissue autofluorescence, so as to obtain the pure spectra of Au–Ft, Dio and DAPI.

3.2. *HE tissue staining of nu/nu kidney sections*

Figure 1 shows the H&E tissue staining on *nu/nu* kidney after Au–Ft administration. The organization structures of renal cortex and medulla were normal compared with control organs without Au–Ft treatment, no hyperplasia or inflammatory infiltration was found in these regions, indicating that Au–Ft treatment did not affect the basic organization structure and functional state of the mice kidney.

3.3. *Fluorescent probe emission spectra*

For defining Au–Ft in cell, we used fluorescent dyes DAPI and Dio to mark cell nucleus and membrane synchronously. However, the emission spectra of both Au–Ft and fluorescent dyes have overlapped with tissue autofluorescence. Blank-labeling and single-labeling tissue sections were prepared to solve this problem. For color coding and spectra deconvolution, emission spectra and tissue autofluorescence data were collected. "Compute pure spectrum" method (patent number: US 6930773 B2) was used on unmixing Au–Ft (Dio or DAPI) signals and tissue autofluorescence, so as to obtain the pure spectra of Au–Ft, Dio and DAPI. As shown in Fig. 2, in particular the excitation wavelength, Au–Ft, DAPI and Dio have their specific emission spectra after deducting the autofluorescence; the emission wavelength of DAPI, Dio and Au–Ft within tissue were 480, 530 and 610 nm, respectively, which were 20–40 nm red shift compared with reagent states.

3.4. *Au–Ft fluorescence imaging at different kidney regions*

Au–Ft possessed the native ferritin's well-defined nanostructure and kidney-specific targeting ability for *nu/nu* mice *in vivo* imaging. Therefore, Au–Ft may hold great promises for some targeted biomedical imaging and diagnosis. Futher studies should be performed on assessing the cellular, subcellular and extracellular localization and quantification of Au–Ft in some cell types of kidney, so as to explore the mechanism of Au–Ft selective enrichment in kidney. Figure 3 showed the fluorescence images of renal cortex and medulla after Au–Ft tail vein injection on *nu/nu* mice at 5 umol/L. To accurately localize the Au–Ft cellular and tissue distribution in kidney, we used specific fluorescence probes to sign the cell membrane (Dio) and nuclei (DAPI) of kidney cells. Note that spectral imaging allowed fluorescence signals to be extracted and highlighted in the deconvolved image. It was found that, in both renal cortex and medulla, Au–Ft was widely

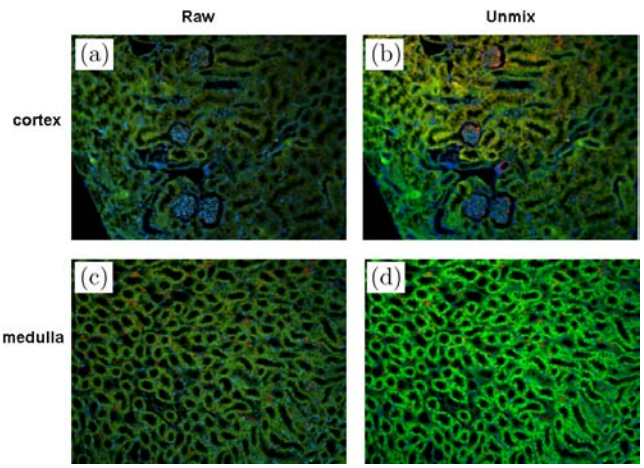

Fig. 3. Fluorescence images of renal cortex and medulla. (a), (c) Raw and (b), (d) processed fluorescence images of kidney cortex (a), (b) and medulla (c), (d) regions after multiplexed fluorescence labeling. The fluorescent probes are DAPI (blue), Dio (green) and Au–Ft (red), as shown in encoded pseudocolors in image (b) and (d). The spectra of each pixel were collected, and "compute pure spectrum" techniques were used to achieve fluorescent signal unmixing and ubiquitous autofluorescence removal.

distributed in extracellular matrix (CECM) and main intracellular region, with no specific location on some specific cellular or tissue regions.

By extracting the signal intensity data from each pixel of image, we could further obtain the quantitative distribution data of Au–Ft in different cellular parts. Figure 4 showed the quantitative distribution of Au–Ft signal in cell membrane, cytoplasm and nuclei of kidney cells after tail vain injection at 5 μmol/L. It was found that, in renal cortex and medulla, the accumulation of Au–Ft in cell membrane and cytoplasm were similar, and both higher than that in nuclei.

Exogenous substances that entered the kidney with blood should undergo a series of metabolism process including glomerulus filtration, tubule reabsorption, and so on. The biodistribution scenes of exogenous substances in kidney is the case we hope to understand. Different doses of Au–Ft (2.8, 4 and 5 μmol/L) were applied on *nu/nu* mice, and their kidney biodistribution profiles were shown in Table 1. The Au–Ft biodistribution properties in cortex and medulla were summarized as follows. (i) Within the cellular region, the accumulation of Au–Ft in cell membrane was more than other positions, the general Au–Ft fluorescence intensity distribution in renal cell was: cell membrane > cytoplasm > nucleus [see Table 1(B)]. This rule applied to both renal cortex and medulla regions, indicating that the Au–Ft maintained relatively strong membrane binding properties. (ii) When the administration dose were 4 μmol/L, Au–Ft accumulated higher in cortex than in medulla; when the administration dose were 2.8 or 5 μmol/L, Au–Ft accumulation in cortex was lower than in medulla [see Table 1(A), $*$]. These results indicated that the Au–Ft concentration in blood might affect their filtration through glomerulus in cortex to get into the tubule in medulla. There existed optimum filtration concentrations for Au–Ft transport in kidney. (iii) In general, when the administration doses were 2.8 or 5 μmol/L, the cellular accumulation of Au–Ft was higher than extracellular matrix [see Table 1(A), §], illustrating that Au–Ft does not always exist as solute in body fluids, it could also be uptaken and bound by renal cells in a considerable amount, so as to enter or pass through the cells by some kind of transcellular translocation; however, when the administration dose of Au–Ft was 4 μmol/L, its cellular accumulation was less than or similar with that in extracellular matrix [see Table (1(A), §]. The lower cell uptake might give an explanation for their limited transfer from renal cortex to renal medulla at this concentration.

The kidney possesses fine internal structures as the basis for its filtration, reabsorption and secretion functions. However, we still do not know by what mechanism the Au–Ft accumulated in kidneys after tail vein injection. The existing research suggested that Au–Ft might be uptaken by renal cells through certain ferritin specific receptors,[1,14,15] but there is no direct evidence at which positions Au–Ft was uptaken and transported in the kidney. So the accurate localization of Au–Ft in kidney will be very conducive to explore the uptake and its interaction with renal cells. In the current study, by using inForm image analysis system, we obtained the fluorescence intensity and cellular location of kidney-targeting Au–Ft on glomerulus and tubules. It is interesting that, the Au–Ft distribution trends within kidney were variable under different treatment doses [see Table 1(A)]. When the Au–Ft content in cells was higher than that of the extracellular matrix (ECM), their accumulation in renal medulla (tubules) was higher than that in cortex (glomerulus) [see Table 1(A)], indicating that cellular uptake constituted the main force for Au–Ft enrichment in medullary tubule and transfer from cortex to medulla. It has been reported that

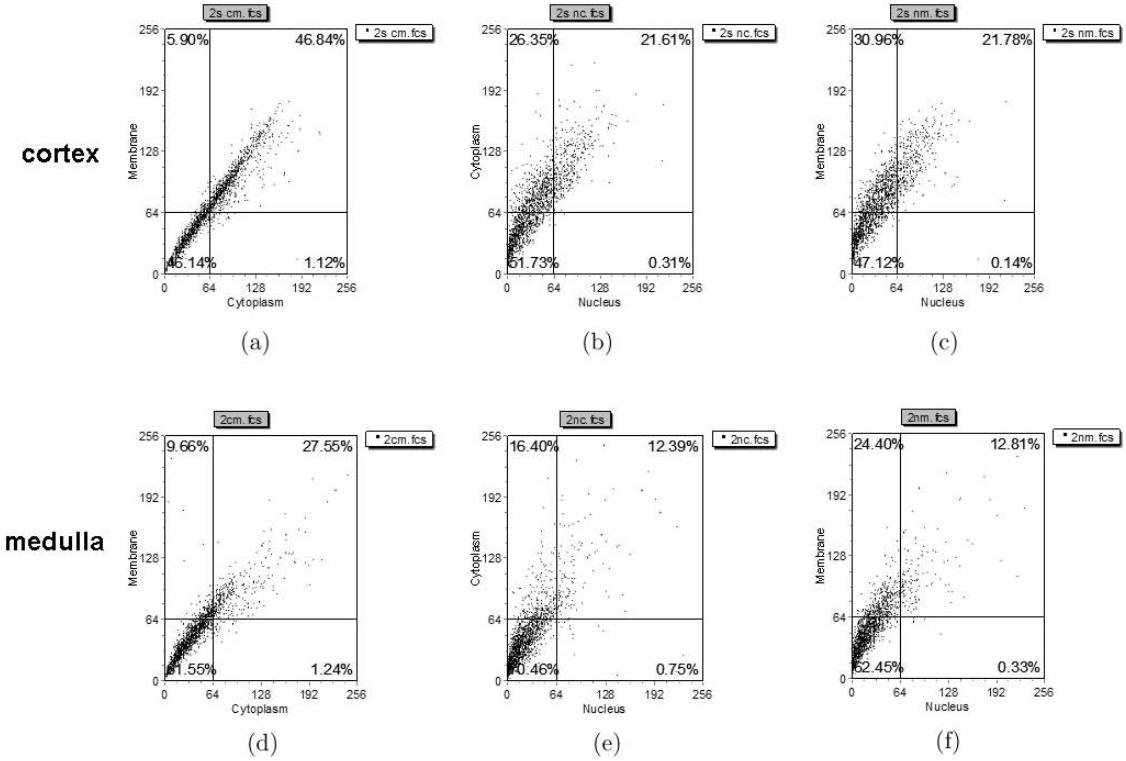

Fig. 4. Au–Ft fluorescence signal at different kidney cell regions. Au–Ft fluorescence signal intensity data were "digitally" extracted from probes staining images of *nu/nu* kidney sections assisted with the colocalization of cell membrane staining (Dio) and nuclei staining (DAPI). (a), (b) and (c) Scatter plots of Au–Ft fluorescence signal distribution among cell membrane, cytoplasm and nuclei of renal cortex cells; (d), (e) and (f) Scatter plots of Au–Ft fluorescence signal distribution among cell membrane, cytoplasm and nuclei of renal medulla cells.

Table 1. The Au–Ft fluorescence signal intensity on kidney sections.

	Renal cortex			Renal medulla		
A	Cell	ECM		Cell	ECM	
Group 1	32.5 ± 11.5§	18.9 ± 9.6		38.8 ± 7.5*,§	31.2 ± 10.9*	
Group 2	57.5 ± 5.7§	127.4 ± 47.3		45.1 ± 14.5*	37.9 ± 11.9**	
Group 3	121.5 ± 10.7§	50.2 ± 12.6		134.4 ± 8.4*,§	94.2 ± 11.3**	
	Renal cortex			Renal medulla		
B	Nucleus	Cytoplasm	Membrane	Nucleus	Cytoplasm	Membrane
Group 1	27.6 ± 12.0	34.2 ± 10.9†	38.9 ± 12.1†	35.1 ± 5.8	39.0 ± 8.6	45.4 ± 8.7†, #
Group 2	39.8 ± 5.6	67.3 ± 5.9‡	71.4 ± 5.9‡, #	32.9 ± 14.5	50.7 ± 14.7†	54.4 ± 14.8†
Group 3	118 ± 11.3	123.5 ± 10.3	128.1 ± 10.7†	125.5 ± 8.0	139.1 ± 7.7†	144.5 ± 11.8†

Au–Ft was administrated on *nu/nu* mice by tail vein injection with the final blood concentration at 2.8 μmol/L (Group 1), 4.0 μmol/L(Group 2) and 5.0 μmol/L(Group 3), respectively. About 5 h after injection, sagittal kidney parafillin section were prepared for imaging and analysis using Nuance system. For one mouse, 2000–2800 cells of cortex or medulla regions were picked from sections for the fluorescence intensity detection. Data presented the fluorescence intensity under the effective exposure time of 1000 ms. Data represent the mean ± SD ($n = 3$ mice per group). (A) Fluorescence signal intensity at renal cells and (ECM). *$p < 0.05$, **$p < 0.01$ compared to the fluorescence signal intensity in the same region (cell or ECM) of renal cortex, §$p < 0.05$ compared to the fluorescence signal intensity of corresponding ECM; (B) Fluorescence signal intensity at different cell compartments of renal cortex and medulla. †< 0.05, ‡$p < 0.01$ compared to the fluorescence signal intensity in nucleus, #$p < 0.05$ compared to the fluorescence signal intensity in cytoplasm. (ANOVA followed by Tukey's test).

proximal tubule cells bind ferritin[14–16] and a receptor for L-subunit ferritin, Scara5, has been identified in proximal tubule during the nephrogenesis. Our data were consistent with these reports and gave a direct image proof that ferritin-coated Au–Ft could be filtrated into crude urine and uptaked by tubule cell. The significant cell membrane enrichment of Au–Ft [see Table 1(B)] indicated the existence of certain membrane receptors responding to Au–Ft uptake. It was further shown that Au–Ft accumulated significantly in cell membrane and was slightly higher than that in cytoplasm, indicating that: (i) Au–Ft targeted-bound to cell membrane was rapidly transported to the cell interior; (ii) As a nanoscaled particle, Au–Ft was uptaken and transferred on renal cell by phagocytosis or pinocytosis. The molecular mechanism and specific pathway by which Au–Ft gets into the cell will be the key problem to thoroughly clarify its renal targeting mechanism.

This study offered a research strategy that the precise localization of a certain fluorescent nanoparticle might be confirmed by the combination of multispectral imaging and multiplexed fluorescent labeling of position-specific probes. The current study provided some important information on Au–Ft tissue biodistribution and cell locations in renal cortex and medulla, which could assist to elucidate the uptake and transport mechanisms of this nanoscale particle in kidney. However, the imaging data from different time points would present a more clear picture on their renal metabolic process.

4. Conclusions

Au–Ft has been proved to be a kidney-targeted fluorescent probe for *in vivo* imaging. Through the combination of multispectral imaging and multiplexed fluorescent labeling of position-specific probes, we could quantitatively analyze Au–Ft fluorescent signal at cell membrane, cytoplasm and nucleus of kidney cell as well as the ECM at both renal cortex and medulla. Our work accurately localized fluorescent nanoparticle Au–Ft in *nu/nu* mice kidney, which provided valuable imaging information for exploring the kidney metabolism and transfer of fluorescent nanoparticle Au–Ft, which maintained potential applications in biological medicine field. This study paved the way for exploring molecular mechanism and specific pathway by which Au–Ft gets into the renal cells, and pointed out the application mode for Au–Ft as a *in vivo* imaging probe.

Acknowledgments

This work was supported by NSFC (31000452; 30900278). H. Y. Gratefully acknowledges the support of Chilong Healthcare International Limited (Beijing) on the using of Nuance multispectral imaging system (CRi, Woburn, MA).

References

1. C. Sun, H. Yang, Y. Yuan *et al.*, "Controlling assembly of paired gold clusters within apoferritin nanoreactor for in vivo kidney targeting and biomedical imaging," *J. Am. Chem. Soc.* **133**, 8617–8624 (2011).
2. X. J. Liang, C. Chen, Y. Zhao, L. Jia, P. C. Wang, "Biopharmaceutics and therapeutic potential of engineered nanomaterials," *Curr. Drug. Metab.* **9** (8), 697–709 (2008).
3. A. E. Farah, "Glucagon and the circulation," *Pharmacol. Rev.* **35**(3), 181–217 (1983).
4. L. S. Weisberg, R. Zanger, "Minerals in dialysis therapy: An introduction," *Semin. Dial.* **23**(6), 547–548 (2010).
5. J. P. Hayslett, "Functional adaptation to reduction in renal mass," *Physiol. Rev.* **59**(1), 137–164 (1979).
6. B. F. Miller, A. Leaf, A. R. Mamby, Z. Miller, "Validity of the endogenous creatinine clearance as a measure of glomerular filtration rate in the diseased human kidney," *J. Clin. Invest.* **31**(3), 309–313 (1952).
7. H. S. Choi, W. Liu *et al.*, "Design considerations for tumour-targeted nanoparticles," *Nat. Nanotechnol.* **5**(1), 42–47 (2010).
8. W. H. De Jong, W. I. Hagens, P. Krystek *et al.*, "Particle size-dependent organ distribution of gold nanoparticles after intravenous administration," *Biomaterials* **29**(12), 1912–1919 (2008).
9. R. Kumar, I. Roy, T. Y. Ohulchanskky *et al.*, "In vivo biodistribution and clearance studies using multimodal organically modified silica nanoparticles," *ACS Nano* **4**(2), 699–708 (2010).
10. M. Li, K. T. Al-Jamal, K. Kostarelos *et al.*, "Physiologically based pharmacokinetic modeling of nanoparticles," *ACS Nano* **4**(11), 6303–6317 (2010).
11. M. A. Rubin, M. P. Zerkowski, R. L. Camp *et al.*, "Quantitative determination of expression of the prostate cancer protein alpha-methylacyl-CoA racemase using automated quantitative analysis (AQUA): A novel paradigm for automated and

continuous biomarker measurements," *Am. J. Pathol.* **164**, 831–840 (2004).
12. A. Psyrri, Z. Yu, P. M. Weinberger *et al.*, "Quantitative determination of nuclear and cytoplasmic epidermal growth factor receptor expression in oropharyngeal squamous cell cancer by using automated quantitative analysis," *Clin. Cancer Res.* **11**, 5856–5862 (2005).
13. R. M. Levenson, A. Fornari, M. Loda, "Multispectral imaging and pathology: Seeing and doing more," *Expert Opin. Med. Diagn.* **2**, 1067–1081 (2008).
14. E. Dimmock, D. Franks, A. M. Glauert, "The location of blood group antigen A on cultured rabbit kidney cells as revealed by ferritin-labelled antibody," *J. Cell Sci.* **10**(2), 525–533 (1972).
15. F. Grinnell, D. C. Hays, "Measurement of anionic sites on the surfaces of baby hamster kidney cells using radiolabeled polycationic ferritin," *Anal. Biochem.* **97**(2), 400–402 (1979).
16. J. Y. Li, N. Paragas, R. M. Ned *et al.*, "Scara5 is a ferritin receptor mediating non-transferrin iron delivery," *J. Dev. Cell* **16**(1), 35–46 (2009).